HHS Public Access

Author manuscript

Acta Biomater. Author manuscript; available in PMC 2020 March 15.

Published in final edited form as:

Acta Biomater. 2019 March 15; 87: 235–244. doi:10.1016/j.actbio.2019.01.073.

Structure-function Relationships of Fetal Ovine Articular Cartilage

Wendy E. Brown[a], **Grayson D. DuRaine**[b], **Jerry C. Hu**[c], and **Kyriacos A. Athanasiou**[d]

[a]Department of Biomedical Engineering, University of California Irvine, 3120 Natural Sciences II Irvine, CA 92697-2715, USA. wendy.brown@uci.edu.

[b]Department of Molecular Microbiology and Immunology, Oregon Health & Science University, 3181 SW Sam Jackson Park Road L220, Portland, OR 97239, USA. duraine@ohsu.edu.

[c]Department of Biomedical Engineering, University of California Irvine, 3120 Natural Sciences II Irvine, CA 92697-2715, USA. jerry.hu@uci.edu.

[d]Department of Biomedical Engineering, University of California Irvine, 3120 Natural Sciences II Irvine, CA 92697-2715, USA. athens@uci.edu.

Abstract

It is crucial that the properties of engineered neocartilage match healthy native cartilage to promote the functional restoration of damaged cartilage. To accurately assess the quality of neocartilage and the degree of biomimicry achieved, its properties must be evaluated against native cartilage and tissue from which the cells for neocartilage formation were sourced. Fetal ovine cartilage is a promising and translationally relevant cell source with which to engineer neocartilage, yet, it is largely non-characterized. The influence of biomechanics during cartilage development, as well as their potential impact on structure-function relationships *in utero* motivates additional study of fetal cartilage. Toward providing tissue engineering design criteria and elucidating structure-function relationships, 11 locations across four regions of the fetal ovine stifle were characterized. Locational and regional differences were found to exist. Although differences in GAG content were observed, compressive stiffness did not vary or correlate with any biochemical component. Patellar cartilage tensile stiffness and strength were significantly greater than those of the medial condyle. Tensile modulus and UTS significantly correlated with pyridinoline content. More advanced zonal organization, more intense collagen II staining, and greater collagen and pyridinoline contents in the trochlear groove and patella suggest these regions exhibit a more advanced maturational state than others. Regional differences in functional properties and their correlations suggest that structure-function relationships emerge *in utero*. These data address the dearth of information of the fetal ovine stifle, may serve as a repository of

Correspondence and reprint requests should be addressed to: Athanasiou, KA, Department of Biomedical Engineering, University of California Irvine, 3120, Natural Sciences II, Irvine, CA 92697-2715 USA, Tel.: (949) 824-9196, Fax: (949) 824-1727, athens@uci.edu.

information for cartilage engineering strategies, and may help elucidate functional adaptation in fetal articular cartilage.

Keywords

Biomechanical; Biochemical; Characterization; Functional Adaptation

1: Introduction

Articular cartilage repair therapies and cartilage tissue engineering efforts aim to restore function to damaged cartilage. To do so, repair cartilages, both innate and engineered, must withstand the arduous loading environments present within articulating joints. The knee, for example, experiences loads up to approximately 3.5 times bodyweight under a combination of compressive, tensile, and shear stresses [1]. Innate repair cartilage naturally formed in response to injuries frequently degenerates because it is mechanically inferior to the surrounding healthy cartilage [2]. Neocartilage has already been generated with not only mechanical properties but also organization that is reminiscent of healthy native tissue [3–5], making neocartilage implantation an appealing treatment for cartilage injuries. The properties of neocartilage may allow it to bear joint loading sooner after surgery than existing treatments, as well as impart the ability of neocartilage to integrate and promote regeneration in both small [6] and large [7] animal models. It is crucial that the properties of repair cartilage match those of the surrounding healthy cartilage to resist degeneration *in situ*, and ultimately, to promote the functional restoration of the injury site.

Histological analysis is frequently employed as the gold standard for assessing the quality of native, repair, and diseased articular cartilages. Indeed, the histological appearance of cartilage is considered to be one of the most important cartilage indicators [8]. To this end, qualitative and semi-quantitative, gross and histological analysis methods have been developed [9–14]. However, mechanical measurements may have greater sensitivity than histology for subtle changes in cartilage quality. Though gross and histological examination may show only subtle differences in cartilage quality, these may reflect large differences in cartilage mechanical properties [15]. It has also been recommended that, regardless of the tissue type being evaluated, e.g., repair cartilage, osteoarthritic cartilage, or engineered neocartilage, histological scores be validated by comparison to quantitative biochemical evaluation [8]. Functionality indices that include both biochemical and mechanical parameters are also used to evaluate the quality of engineered neocartilages and degree to which native tissue properties, or biomimicry, are achieved [3, 16]. To determine the biomimicry achieved, and thus, the quality of engineered and repair cartilages, they must be assessed against healthy native cartilage by a complete set of histological and quantitative parameters, including biochemical, and mechanical assessments.

To accurately assess the quality of and the biomimicry achieved by repair cartilage, it is essential to characterize healthy native cartilage of the relevant animal model. Native cartilage functional properties vary greatly with factors, such as species, age, and location. For example, the aggregate modulus of the adult bovine lateral condyle greatly exceeds that

of an adult rabbit, but the aggregate modulus of the adult leporine trochlear groove exceeds that of the adult cow [17]. Equine models exhibit age-dependent and topographical changes in mechanical properties [18]. A common translational model for cartilage repair, the ovine stifle, shows significant differences in both biochemical content and mechanical properties across different regions [19]. With the translational use of the ovine model in mind, fetal ovine cartilage is emerging as highly promising cell source for cartilage engineering, since fetal chondrocytes have high proliferative and matrix synthesis abilities [20, 21]. However, there is a dearth of knowledge of the quantitative functional properties of the fetal ovine stifle. While the fetal sheep is not used as an *in vivo* model for cartilage repair, it is necessary to understand the properties of fetal ovine cartilage to evaluate the quality of neocartilage engineered from this source and degree of biomimicry achieved. The first step to quantitatively evaluating biomimicry is to compare engineered tissues to the target tissue which they will replace. For example, neocartilage engineered with fetal ovine chondrocytes may be evaluated against healthy juvenile or adult ovine cartilage surrounding a defect. However, it is always instructive to also evaluate engineered neocartilage against the source from which cells were obtained to evaluate the degree to which the native tissue was recapitulated. Thus, the functional properties of the fetal ovine articular cartilage must be known. To provide benchmark functional properties to allow for the evaluation of biomimicry of engineered neocartilage, it is necessary to characterize multiple locations within the articular cartilage of the species and age of animal model used, such as the translationally relevant fetal ovine stifle.

Cartilage biomechanics throughout development and maturation drive the emergence of topographical and regional variations in cartilage properties. The *in utero* mechanical environment acts as a regulator of stem cell fate and contributes to chondrogenesis and skeletogenesis. The balance of hydrostatic pressure, intermittent strain, and shear stresses direct the progression of the cartilage ossification front [22]. Biomechanical forces also promote cartilage maturation throughout fetal development and after birth. While cartilage mechanical properties are generally thought to change with developmental stage, loading patterns also drive topographical variations of functional properties in a process referred to as functional adaptation. For example, newborn and adult cartilage exhibits increased stiffness in areas bearing greater loads [18]. It has also been shown that cartilage from regions of the adult ovine stifle joints subjected to differing mechanical stresses contains chondrocyte populations of different phenotypes, as indicated by their relative synthesis of biglycan and decorin [23]. Several studies have shown that fetal cartilage is “blank,” [18, 24, 25] i.e., regional variations in biochemical content or mechanical properties were not detected. However, these studies are limited by the examination of only a few regions or by employing either histological examination, biochemical quantification, or mechanical analyses, but not all of them comprehensively. The importance and role of biomechanical stimuli in the development of articular cartilage *in utero* suggests these forces may also contribute to the cartilage’s early functional adaptation, motivating a comprehensive examination of fetal cartilage properties.

While structure-function relationships in native adult cartilage are well-studied, many of these relationships have yet to be elucidated for fetal-aged cartilage. Differences in structure-function relationships between fetal and adult cartilage would further suggest a role for

functional adaptation. Additionally, identifying correlations between mechanical properties and biochemical content within native fetal cartilage may inform the development of non-destructive cartilage evaluation methods. For example, an optical tool has recently been developed to nondestructively obtain cartilage mechanical properties by measuring proteoglycan and collagen contents, then using these data and structure-function correlations to yield compressive and tensile properties [26]. Comprehensive characterization of fetal ovine stifle cartilage may shed light on the influence of biomechanical stimuli on cartilage developmental processes and functional adaptation.

The objectives of this study were three-fold: 1) To provide a benchmark for the evaluation of quality and biomimicry in cartilage engineering efforts that utilize fetal ovine cell sources, 2) to identify correlations between mechanical properties and biochemical contents toward elucidating structure-function relationships in fetal ovine cartilage, and 3) to provide missing data on the translationally relevant fetal ovine stifle, which may help elucidate functional adaptation of knee cartilage. This was accomplished by topographical and regional characterization of the articular cartilage of the fetal ovine stifle, including a comprehensive array of histological, biochemical, and mechanical assays. It was expected that characterizing 11 locations across four regions (medial condyle, lateral condyle, trochlear groove, and patella) of the fetal ovine stifle would elucidate variations reflecting the influences of the biomechanical environment present during native cartilage formation.

2: Materials and Methods

2.1: Native Tissue Sample Preparation

The stifle joints of fetal (day 120 of ~150 day gestation) Dorper cross sheep were obtained as medical waste from the UC Davis School of Veterinary Medicine (Davis, CA) the day of sacrifice (n = 6). Each joint was divided into topographical locations across four regions of the stifle (Figure 1). Specifically, the stifle was first divided into the medial condyle, lateral condyle, trochlear groove, and patella. Subsequently, each region was subdivided into topographical locations; e.g., the medial condyle was divided into three sections. Samples for all testing methods were removed from the middle portion of each location and were immediately mechanically tested or preserved for histology. Additional samples from these locations were weighed and frozen for biochemical analysis. Samples were isolated from three locations on the medial condyle (MC), three locations on the lateral condyle (LC), three locations on the trochlear groove (TG), and two locations on the patella (P) by taking 5 mm diameter punches from each location. These punches were then trimmed to a uniform thickness of 2.5 mm, with the articular surface intact, using a jig. Samples for compression testing were isolated by coring out a 3 mm diameter disc from the center of the 5 mm punch. Tensile samples were taken from the periphery of the remaining annulus. The residual tissue not used for mechanical testing was then apportioned for histological and biochemical assays. Separate from the fetal tissues analyzed, juvenile ovine cartilage samples for the evaluation of crosslinks were obtained be removing the cartilage from the subchondral bone with a dermatome and trimming the pieces to uniform size, approximately 3 × 3 mm.

2.2: Gross Morphological Analysis

The exact dimensions of the stifle joint and cartilage samples were measured using ImageJ software (NIH) from photographs taken during sample preparation. Joint measurements were taken at the longest and/or widest points of each region.

2.3: Histological Evaluation

After fixation in 10% neutral buffered formalin, cartilage samples were dehydrated, embedded in paraffin, and sectioned to a thickness of 4 μm to expose the full thickness of the tissue. Sections were stained with Hematoxylin and Eosin to illustrate tissue and cell morphology, Safranin O/Fast Green to visualize glycosaminoglycans (GAGs), and Picrosirius Red to visualize collagen. Immunohistochemistry was also used to visualize collagen I (ab34710, 1:250 dilution, Abcam) and collagen II (ab34712, 1:4000 dilution, Abcam). The presence of vascularization was detected and its distance from the articular surface was measured using ImageJ from Picrosirius Red-stained slides of each topographical location.

2.4: Biochemical Characterization

Samples were weighed to obtain wet weights, frozen and lyophilized, and weighed again to obtain dry weights. Lyophilized samples were digested in 125 μg/mL papain in phosphate buffer at 60° C for 18 hours and assayed to determine biochemical content. A Blyscan dimethyl methylene blue assay kit (Biocolor, Ltd) was used to measure sulfated GAG content in the samples. A modified colorimetric chloramine-T hydroxyproline assay using hydrochloric acid [27] and a Sircol collagen assay standard (Biocolor, Ltd) was used to quantify collagen content. DNA content was measured by performing a Picogreen assay (Quant-iT Picogreen dsDNA assay kit). GAG and collagen contents were normalized to wet weight, dry weight, and DNA. High-performance liquid chromatography (HPLC) was performed to quantify pyridinoline crosslinks within fetal ovine cartilage, as well as juvenile ovine cartilage for reference. Lyophilized samples were digested in 4N HCl and dried in a vacuum concentrator. Digested samples were resuspended in 500 μL of a solution containing 1.67 nmol pyroxidine/mL, 8.3% acetonitrile, and 0.41% heptafluorobutyric acid (HFBA) in water. Resuspended samples were injected into a 25 mm C18 column (Shimadzu) and eluted using a modified solvent profile consisting of two solvents (1: 24% methanol and 0.13% HFBA in water and 2: 75% acetonitrile and 0.1% HFBA in water) [28]. Pyridinoline crosslinks were normalized to wet weight and total collagen content.

2.5: Mechanical Characterization

Creep indentation testing was performed by applying a 0.9 mm diameter, flat, porous indenter tip to the center of the 3 mm cylindrical cartilage punches under a 0.5 N load via an automated system, which resulted in 8–10% sample strain. Creep compression was determined by continuously measuring the indenter position [1, 29]. Values for the aggregate modulus, shear modulus, and permeability were obtained from the experimental data using a semi-analytical, semi-numerical, linear biphasic model and finite element analysis [29]. Uniaxial tensile testing was also performed. Using a jig, 5 mm-diameter cartilage annuli remaining after compression sample isolation were trimmed into 1 mm thick layers still

containing the articular surface. Dog bone-shaped specimens with the long axis in the direction of joint articulation and a gauge length of 2.34 mm were isolated from the trimmed annuli, in adherence with ASTM standards (ASTM D3039). Paper tabs were glued to the specimens outside the gauge length and gripped in a TestResources uniaxial tester (TestResources Inc). The tabs were pulled parallel to the long axis of the specimen at a rate of 1% of the gauge length per second until sample failure. A nominal stress-strain curve was generated using the cross-sectional area of samples measured with ImageJ. A least-squares fit of the linear region of the curve yielded the tensile modulus and the maximum nominal stress achieved yielded the ultimate tensile strength (UTS).

2.6: Statistical Analysis

One-way analysis of variance tests (ANOVAs) followed by Tukey's post hoc tests were performed using Prism 7 software (GraphPad) on the quantitative data comparing the three topographical locations within each of the medial condyle, lateral condyle, and trochlear groove. Student's t-tests were performed comparing the two topographical locations on the patella. One-way ANOVAs with Tukey's post hoc tests were performed on the combined data from each region to compare data across the medial condyle, lateral condyle, trochlear groove, and patella regions. Two-way ANOVAs with Tukey's post hoc tests were used to analyze pyridinoline/wet weight and pyridinoline/collagen regional data. Correlations between mechanical properties (aggregate modulus, tensile modulus, and UTS) and biochemical contents (GAG/wet weight, collagen/wet weight, pyridinoline/wet weight, and pyridinoline/collagen) matched by location were detected by calculating Pearson correlation coefficients. Significance for all statistical analyses was determined by $p < 0.05$. Significantly different groups are indicated in figures by labeling with different letters.

3: Results

3.1: Gross Morphology

All cartilage appeared glossy and opaque white with visible vasculature underneath the translucent cartilage (Figure 1). The medial condyle was 39 ± 2 mm long and 16 ± 1 mm wide. The lateral condyle was 40 ± 1 mm long and 17 ± 1 mm wide. The trochlear groove was 46 ± 3 mm long and 26 ± 0 mm wide. The patella was 42 ± 1 mm long and 30 ± 1 mm wide.

3.2: Histology

Histological and immunohistochemical staining is shown in Figure 2. Histologically, a large portion of the joint appeared to be cartilaginous. A tidemark or calcified osteochondral transitional region was not present, therefore it was not possible to accurately measure cartilage thickness. All topographical locations were densely populated with chondrocytes and showed vasculature. In the MC1, MC2, and MC3 locations, vascularization was present 668 ± 157, 485 ± 10, and 558 ± 219 μm below the surface, respectively. In the LC1, LC2, and LC3 locations, vascularization was present 496 ± 147, 519 ± 17, and 488 ± 82 μm below the articular surface, respectively. In the TG1, TG2, and TG3 locations, vascularization was present 490 ± 119, 596 ± 49, and 496 ± 28 μm below the articular surface, respectively. In the P1 and P2 locations, vascularization was present 485 ± 36 and 518 ± 10 μm below the

articular surface, respectively. Chondrocytes near the articular surface were elongated with their long axis parallel to the surface and organized as single cells spaced 20–30 μm apart. Approximately 50 μm below the surface, chondrocytes appeared rounded and remained as individual cells or pairs of cells in close proximity (5–10 μm) to each other. Individual cells or pairs were spaced 20–30 μm apart with random organization. Within approximately 100–800 μm below the surface, chondrocytes appeared as either individual cells or pairs of cells within lacunae, and the space between single or paired cells increased to 40–50 μm, with some large gaps up to 80 μm. Beyond approximately 800 μm below the articular surface, cell density increased, and lacunae became larger. The presence of more distinct zones and large lacunae containing multiple chondrocytes were most evident in the patella and trochlear groove than in the medial or lateral condyle.

At all topographical locations, GAG staining was faint near the articular surface but increased with cartilage depth. Regionally, the lateral condyle stained most intensely for GAG, followed by the medial condyle, trochlear groove, and patella. Within each region, the locations with the most intense GAG staining were MC3, LC2, TG1, and P1, respectively. Total collagen staining was intense at the articular surface, faint below the surface, and more intense with increasing tissue depth for all locations. Collagen staining was similar between the medial and lateral condyle and slightly less intense in the patella. Collagen staining of the trochlear groove appeared much less intense than the other regions. Within the medial condyle, lateral condyle, trochlear groove, and patella, collagen staining was most intense at the MC2, LC2, TG1, and P2 locations, respectively. All locations stained minimally for collagen I, with the most intense staining occurring at the articular surface. All locations stained positively for collagen II, but with varying intensities. The trochlear groove stained most intensely for collagen II, followed by the medial condyle, lateral condyle, and patella. Within the medial condyle, lateral condyle, trochlear groove, and patella, collagen II staining was most intense at the MC2, LC3, TG1, and P1 locations, respectively. The distribution of GAG and collagen, as well as the cellular shape and organization observed in the present study mirrors matrix distribution and cellular organization observed in mature articular cartilage, suggesting the presence of precursor cartilage zones in fetal ovine articular cartilage.

3.3: Biochemical Content

A topographical analysis of biochemical content within each region is shown in Table 1. Notably, the GAG/DNA content of the MC3 location was significantly greater than that of the MC1 location. The GAG/wet weight content of the TG1 location was significantly greater than that of the TG3 location. GAG/dry weight contents of the MC1, MC2, and MC3 locations were 27 ± 5, 30 ± 4, and 33 ± 8%, respectively. GAG/dry weight contents of the LC1, LC2, and LC3 locations were 34 ± 7, and 37%, respectively. GAG/dry weight contents of the TG1, TG2, and TG3 locations were 36 ± 9, 33 ± 6, and 32 ± 15%, respectively. GAG/dry weight contents of the P1 and P2 locations were 33 ± 9 and 28 ± 3%, respectively. Collagen/dry weight contents of the MC1, MC2, and MC3 locations were 54 ± 8, 57 ± 12, and 52 ± 7%, respectively. Collagen/dry weight contents of the LC1, LC2, and LC3 locations 63 ± 20, 68 ± 25, and 58 ± 11%, respectively. Collagen/dry weight contents of the

TG1, TG2, and TG3 locations were 45 ± 8, 47 ± 9, and 52 ± 13%, respectively. Collagen/dry weight contents of the P1 and P2 locations were 57 ± 7 and 62 ± 15%, respectively.

A regional comparison of biochemical content is shown in Figure 3 in gray. Historical data regarding regional biochemical content of juvenile ovine articular cartilage is also included in translucent blue. Collagen/dry weight contents in the patella and lateral condyle were significantly greater than that of the trochlear groove. Additionally, a topographical examination of pyridinoline crosslinks within juvenile ovine articular cartilage was performed for reference. Pyridinoline/wet weight contents of the juvenile ovine MC1, MC2, and MC3 locations were 197 ± 8, 148 ± 14, and 171 ± 11 nmol/g, respectively. The pyridinoline/wet weight content of the MC1 location significantly exceeded that of the MC2 location. Pyridinoline/wet weight contents of the juvenile ovine LC1, LC2, and LC3 locations were 191 ± 45, 253 ± 44, and 159 ± 6 nmol/g, respectively. Pyridinoline/wet weight contents of the juvenile ovine TG1, TG2, and TG3 locations were 224 ± 16, 263 ± 119, and 250 ± 57 nmol/g, respectively. Pyridinoline/wet weight contents of the juvenile ovine P1 and P2 locations were 331 ± 84 and 200 ± 27 nmol/g, respectively. Pyridinoline/collagen contents of the juvenile ovine MC1, MC2, and MC3 locations were 1.1 ± 0.1, 0.9 ± 0.2, and 1.4 ± 0.3 nmol/mg, respectively. Pyridinoline/collagen contents of the juvenile ovine LC1, LC2, and LC3 locations were 1.1 ± 0.3, 1.8 ± 0.5, and 1.3 ± 0.5 nmol/mg, respectively. Pyridinoline/collagen contents of the juvenile ovine TG1, TG2, and TG3 locations were 3.2 ± 2.1, 1.8 ± 0.8, and 1.7 ± 0.7 nmol/mg, respectively. Pyridinoline/collagen contents of the juvenile ovine P1 and P2 locations were 1.5 ± 0.7 and 1.9 ± 0.2 nmol/mg, respectively.

3.4: Mechanical Properties

A topographical analysis of mechanical properties within each region is shown in Table 2. A regional comparison of mechanical properties is shown in Figure 4. Historical data regarding regional mechanical properties of juvenile ovine articular cartilage is also included in translucent blue.

3.5: Structure-Function Relationships

Statistical correlations between mechanical properties (aggregate modulus, tensile modulus, and UTS) and biochemical contents (GAG/wet weight, collagen/wet weight, pyridinoline/wet weight, and pyridinoline/collagen) to identify structure-function relationships (Figure 5). Tensile modulus significantly correlated positively with pyridinoline/wet weight and pyridinoline/collagen contents. UTS significantly correlated positively with collagen/wet weight, pyridinoline/wet weight, and pyridinoline/collagen contents.

4: Discussion

The goals of this study were to establish missing quantitative benchmark data for the evaluation of biomimicry in cartilage engineering efforts that use fetal ovine chondrocytes and to identify structure-function relationship in the cartilage. This was accomplished by comprehensively characterizing the articular cartilage of the fetal ovine stifle. Despite the

prominence of the ovine model for translational cartilage repair and tissue engineering studies, as well as the emerging use of fetal chondrocytes for cartilage engineering, the fetal ovine stifle has not yet been examined [30]. The hypothesis that locational or regional differences in fetal ovine cartilage properties would exist was supported by the data; significant differences among anatomical regions were observed histologically, biochemically, and mechanically (Figures 2, 3, 4). Furthermore, significant differences in biochemical content and mechanical properties were observed among topographical locations within regions (Tables 1 and 2). To identify structure-function relationships, statistical tests for correlations between biochemical and mechanical data were performed. Tensile properties were observed to significantly correlate with pyridinoline contents (Figure 5). In contrast to prior work in fetal bovine and equine models, regional patterns of biochemical and mechanical properties of fetal ovine cartilage were observed to match those previously reported for ovine cartilage of older animals [19]. The sequence of development of extracellular matrix (ECM) components and mechanical properties parallels that seen during *in vitro* cartilage formation [2]. This study represents the first comprehensive characterization of fetal cartilage. Additionally, as the first effort to examine the articular cartilage of fetal ovine stifle, these data serve as a basis for evaluating the quality of cartilages engineered from this cell source. These data address the dearth of knowledge of the fetal ovine stifle and yield new perspectives on the development of structure-function relationships, functional adaptation, and maturation of articular cartilage.

Correlations between compressive stiffness and individual biochemical contents are not evident in fetal ovine cartilage, but such structure-function relationships may become clear with the further development and interaction of matrix components. Ovine articular cartilage in the mid-third trimester was observed to contain GAG content on par with juvenile ovine articular cartilage (Figures 4) [19]. Uniformity of GAG content throughout life has also been observed in other large quadruped animals, such as bovine and equine models [24, 31]. GAG content is the main component thought to impart compressive stiffness to cartilage [32]. Therefore, GAG uniformity may exist because joints experience compressive forces *in utero* [22] and must be able to bear load after birth, as lambs attempt to stand immediately to nurse. It is also important to note that while the loads articular cartilage experiences may be low compared to adult animals, the stresses experienced remain high because of smaller cartilage surface area in younger animals. This study shows, for the first time, regional and locational differences in GAG content of fetal articular cartilage (Figure 3 and Table 1). In contrast, fetal compressive stiffness was found not to vary. Compressive stiffness may also be influenced by other factors, such as genetics, collagen [24] and pyridinoline crosslink contents [33], and the interaction of matrix components [34, 35]. Therefore, the lack of correlation between the aggregate modulus of fetal ovine cartilage with matrix components (Figure 5) may be because collagen and pyridinoline contents are still well below levels seen in juvenile and adult ovine cartilage [19]. The larger mechanical forces experienced by articular cartilage after birth may stimulate cartilage maturation by production of collagen and pyridinoline [36, 37], and subsequently allow for matrix interactions that more clearly define functional relationships between compressive stiffness and biochemical contents.

In contrast to the absence of compressive structure-function relationships, tensile structure-function relationships in fetal ovine cartilage are evident in this study. Prior studies have

shown that mechanical properties and biochemical content of equine and bovine fetal and neonatal cartilage do not differ among locations [18, 24, 25]. However, in this study, the tensile modulus and UTS values of the fetal patella were 73% and 65% greater than those of the medial condyle (Figure 4). It is possible that differences in functional properties are more evident in this study because of the greater number of locations examined than previous studies (11 versus two). While collagen content is considered to be the main contributor to tensile properties, it has been shown that the degree of pyridinoline crosslinking within the collagen network also greatly contributes to tensile properties [38–40]. Despite the collagen and pyridinoline contents of fetal ovine cartilage (Figure 3) being an order of magnitude lower than in juvenile cartilage [19], significant, positive correlations were found between tensile modulus and both pyridinoline/wet weight and pyridinoline/collagen contents. Furthermore, UTS significantly correlated positively with pyridinoline/collagen content (Figure 5). Sub-mature levels of collagen and pyridinoline contents in fetal bovine cartilage, as well as significant, positive correlations between tensile properties and these matrix components have also been shown in bovine cartilage from pooled ages [25]. However, these correlations were not detected within only fetal-aged bovine cartilage. This implies that the mechanical stimulation experienced by ovine cartilage *in utero* elicits functional adaptation much earlier than previously thought [18, 41]. While this is not the first time that crosslinking has been explored in fetal cartilage [24, 25], this study represents the first examination of these characteristics in fetal ovine cartilage, the first evidence to suggest functional adaptation *in utero*, and the first time pyridinoline-related maturation has been shown to vary regionally within a developing joint. These data may serve to inform future studies of chondrocyte function in functional adaptation, such as the temporal endogenous expression of collagen crosslinking enzymes. Clearly defined structure-function relationships between tensile properties and pyridinoline crosslinks suggest that functional adaptation of cartilage occurs much earlier than previously thought.

In addition to the presence of locational and regional differences in biochemical and mechanical properties within fetal ovine articular cartilage, region-based, maturational differences were also observed. While no tidemark was present, the precursors of cartilage zones were observed (Figure 2), being most defined in the patella and trochlear groove. Collagen II staining was most intense in the trochlear groove and patella. During cartilage development, other collagens, such as type VI [42, 43], are prevalent within the bulk of fetal cartilage and localize to the pericellular matrix prior to increased collagen II production [43]. Therefore, the bulk of collagen staining in other regions may be due to collagen VI. The more advanced development of cartilage zones and the presence of intense collagen II staining in the trochlear groove and patella suggest that these regions are the first to mature, and, for the first time, suggest that different regions of the fetal knee exhibit different degrees of cartilage maturation. It is known that biomechanics have profound effects *in utero* [22, 44, 45]. The progression of the ossification front [22] is known to be dictated by the balance of hydrostatic pressure, which increases the production of aggrecan and collagen II [46], with tensile and shear strain, which are associated with endochondral ossification [46, 47]. When hydrostatic stress and shear stress simulations were applied to computer models of a diarthrodial joint, an osteogenic center was predicted to appear closer to the surface in a concave joint surface [46], i.e., the trochlear groove. This is in contrast to when simulations

were applied to a concave joint surface, i.e. the femoral condyles, where the osteogenic center appeared deeper within tissue. This supports the observation in this study that the trochlear groove and the opposing patella exhibit advanced maturation compared to other regions. The balance of biomechanical forces cartilage experiences *in utero* which drive endochondral ossification and cartilage maturation also may provide further evidence that the trochlear groove and patella regions mature first.

By combining the data obtained in this study with previous studies of cartilage in older animals, it may be possible to delineate cartilage maturation pathways. In terms of the development of cartilage ECM components, GAG content may be established first. In this study, GAG content at the mid-third trimester was observed to be on par with that of juvenile cartilage [19]. The abundance of GAG imparts compressive stiffness to fetal cartilage that is on the same order of magnitude as juvenile cartilage [19]. Despite mature levels of GAG content, collagen and pyridinoline contents in fetal cartilage were well below those previously reported for juvenile ovine cartilage [19]. Next to develop in the ECM may be collagen, followed by pyridinoline. Collagen and pyridinoline contents have been shown to increase through 2 years of age in bovine articular cartilage [25]. After collagen synthesis and collagen fiber assembly, lysyl oxidase (LOX), a collagen crosslinking enzyme, may induce the formation of pyridinoline crosslinks between collagen fibers, stabilizing the formation of heterotypic fibers, and therefore the ECM as a whole [40]. Concomitant with the increase in crosslinking is an increase in cartilage tensile properties [25]. In this study, significant correlations between tensile properties and pyridinoline contents were detected. This is likely due to the strong contribution of crosslinking to cartilage tensile properties, versus the contribution of multiple matrix components to compressive properties. By combining the insights gained from this work with previous studies of cartilage development, a clearer picture of the sequence of events that give rise to cartilage's salient properties emerges.

Scaffold-free cartilage tissue engineering methods are reminiscent of the cartilage developmental progressions elucidated in the present study. Articular cartilage engineered with the self-assembling process develops in phases [48]. In the first phase, cells are seeded at a high density into non-adherent agarose wells to prevent cellular adhesion to the substrate and encourage cellular interactions. This phase is reminiscent of mesenchymal condensation that takes place during developmental chondrogenesis [49]. In the second phase, free energy is minimized as N-cadherin-mediated cell-to-cell interactions take place, resulting in neocartilage formation. In native cartilage development, N-cadherin plays an important role in early condensation [50]. In the third phase, collagen VI and high levels of GAG, specifically chondroitin-6-sulphate, are synthesized [48]. GAG levels increase to native-tissue levels and plateau within 4 weeks [51]. Similarly, this study and other show that GAG content within fetal cartilage is established early, as levels *in utero* are on par with juvenile cartilage [19, 24]. In the fourth phase of self-assembly, collagen VI localizes to the pericellular matrix, collagen II production increases, and chondroitin-6-sulphate:chondroitin-4-sulphate ratio decreases, all paralleling developmental processes [31, 42, 43, 51, 52]. These biochemical components impart a nascent level of compressive and tensile characteristics in engineered neocartilage; however, collagen content and pyridinoline crosslinking remain below the levels of mature native tissue [19, 25, 39]. This implies that

neocartilage engineered with this method has yet to complete maturation. Recently identified structure-function relationships show the importance of pyridinoline crosslinks to not only tensile properties but also compressive properties [24, 25, 39]. The exogenous treatment of neocartilage with lysyl oxidase-like 2 (LOXL2), a LOX homolog enzyme that creates pyridinoline crosslinks within the collagen network, may recapitulate pyridinoline-associated maturation in native cartilage development [40]. The “order of operations” of cartilage development elucidated in this study is replicated in neocartilage development, often to native cartilage levels, lending further credence to the self-assembling process as an *in vitro* model of cartilage formation and development.

In summary, this study yielded a quantitative understanding of the articular cartilage of the fetal ovine stifle, and in doing so, elucidated the development of structure-function relationships and suggesting new perspectives on functional adaptation. It was shown that fetal cartilage exhibits locational and regional variations in histological, biochemical, and mechanical properties. In general, the GAG content and aggregate modulus of fetal cartilage were on par with those of juvenile cartilage. No significant structure-function correlations could be identified between aggregate modulus and any biochemical component within fetal cartilage. While collagen content, pyridinoline content, and tensile properties of fetal cartilage were much lower than in more mature cartilage, clear structure-function relationships were illustrated with respect to tensile properties. Tensile modulus and UTS were correlated to pyridinoline content, further supporting recent evidence that not only collagen content, but also crosslinking greatly contributes to tensile properties. These data suggest that functional adaptation in articular cartilage begins *in utero*, much earlier than previously thought, potentially as a product of the forces that drive endochondral ossification. The trochlear groove and patella exhibited the greatest tensile properties and most intense collagen II staining, providing evidence of a more advanced maturation in these areas. These observations, combined with previously reported studies of cartilage development, may clarify the order of development of cartilage functional properties and further substantiate the self-assembling process as an *in vitro* model of cartilage development. These data also serve as a repository of information for fetal ovine cartilage, providing benchmark functional properties for tissue engineering efforts.

Acknowledgments

This work was supported by the National Institutes of Health R01 AR067821. The authors would also like to thank Drs. Diana Farmer, Aijun Wang, and Gary Raff for the generous donation of the fetal ovine stifle joints and Linda Talken for assistance in obtaining the tissues.

The sponsor of this work had no role in the study design, the collection, analysis, and interpretation of data, writing of the report, or the decision to submit this article for publication.

References

[1]. Mow VC, Gibbs MC, Lai WM, Zhu WB, Athanasiou KA, Biphasic indentation of articular cartilage--II. A numerical algorithm and an experimental study, J Biomech 22(8–9) (1989) 853–61. [PubMed: 2613721]

[2]. Athanasiou KA, Darling EM, DuRaine GD, Hu JC, Reddi AH, Articular Cartilage, Second ed., CRC Press, Boca Raton, FL, 2017.

[3]. MacBarb RF, Chen AL, Hu JC, Athanasiou KA, Engineering functional anisotropy in fibrocartilage neotissues, Biomaterials 34(38) (2013) 9980–9. [PubMed: 24075479]

[4]. Zhu D, Tong X, Trinh P, Yang F, Mimicking Cartilage Tissue Zonal Organization by Engineering Tissue-Scale Gradient Hydrogels as 3D Cell Niche, Tissue engineering. Part A 24(1–2) (2018) 1–10. [PubMed: 28385124]

[5]. Steele JA, McCullen SD, Callanan A, Autefage H, Accardi MA, Dini D, Stevens MM, Combinatorial scaffold morphologies for zonal articular cartilage engineering, Acta Biomater 10(5) (2014) 2065–75. [PubMed: 24370641]

[6]. DuRaine GD, Arzi B, Lee JK, Lee CA, Responte DJ, Hu JC, Athanasiou KA, Biomechanical evaluation of suture-holding properties of native and tissue-engineered articular cartilage, Biomech Model Mechanobiol 14(1) (2015) 73–81. [PubMed: 24848644]

[7]. Mainil-Varlet P, Rieser F, Grogan S, Mueller W, Saager C, Jakob RP, Articular cartilage repair using a tissue-engineered cartilage-like implant: an animal study, Osteoarthr Cartilage 9 (2001) S6–S15.

[8]. Rutgers M, van Pelt MJ, Dhert WJ, Creemers LB, Saris DB, Evaluation of histological scoring systems for tissue-engineered, repaired and osteoarthritic cartilage, Osteoarthritis and cartilage / OARS, Osteoarthritis Research Society 18(1) (2010) 12–23.

[9]. O'Driscoll SW, Keeley FW, Salter RB, The chondrogenic potential of free autogenous periosteal grafts for biological resurfacing of major full-thickness defects in joint surfaces under the influence of continuous passive motion. An experimental investigation in the rabbit, The Journal of bone and joint surgery. American volume 68(7) (1986) 1017–35. [PubMed: 3745239]

[10]. Pineda S, Pollack A, Stevenson S, Goldberg V, Caplan A, A semiquantitative scale for histologic grading of articular cartilage repair, Acta Anat (Basel) 143(4) (1992) 335–40. [PubMed: 1502876]

[11]. Smith GD, Taylor J, Almqvist KF, Erggelet C, Knutsen G, Garcia Portabella M, Smith T, Richardson JB, Arthroscopic assessment of cartilage repair: a validation study of 2 scoring systems, Arthroscopy : the journal of arthroscopic & related surgery : official publication of the Arthroscopy Association of North America and the International Arthroscopy Association 21(12) (2005) 1462–7.

[12]. Mainil-Varlet P, Van Damme B, Nesic D, Knutsen G, Kandel R, Roberts S, A new histology scoring system for the assessment of the quality of human cartilage repair: ICRS II, Am J Sports Med 38(5) (2010) 880–90. [PubMed: 20203290]

[13]. O'Driscoll SW, Marx RG, Beaton DE, Miura Y, Gallay SH, Fitzsimmons JS, Validation of a simple histological-histochemical cartilage scoring system, Tissue engineering 7(3) (2001) 313–20. [PubMed: 11429151]

[14]. Grogan SP, Barbero A, Winkelmann V, Rieser F, Fitzsimmons JS, O'Driscoll S, Martin I, Mainil-Varlet P, Visual histological grading system for the evaluation of in vitro-generated neocartilage, Tissue engineering 12(8) (2006) 2141–9. [PubMed: 16968155]

[15]. Waldstein W, Perino G, Gilbert SL, Maher SA, Windhager R, Boettner F, OARSI osteoarthritis cartilage histopathology assessment system: A biomechanical evaluation in the human knee, J Orthop Res 34(1) (2016) 135–40. [PubMed: 26250350]

[16]. Elder BD, Athanasiou KA, Systematic assessment of growth factor treatment on biochemical and biomechanical properties of engineered articular cartilage constructs, Osteoarthr Cartilage 17(1) (2009) 114–123.

[17]. Athanasiou KA, Rosenwasser MP, Buckwalter JA, Malinin TI, Mow VC, Interspecies comparisons of in situ intrinsic mechanical properties of distal femoral cartilage, J Orthop Res 9(3) (1991) 330–40. [PubMed: 2010837]

[18]. Brommer H, Brama PA, Laasanen MS, Helminen HJ, van Weeren PR, Jurvelin JS, Functional adaptation of articular cartilage from birth to maturity under the influence of loading: a biomechanical analysis, Equine Vet J 37(2) (2005) 148–54. [PubMed: 15779628]

[19]. Huwe LW, Brown WB, Athanasiou KA, Hu JC, Characterization of costal cartilage and its suitability as a cell source for articular cartilage tissue engineering.

[20]. Choi WH, Kim HR, Lee SJ, Jeong N, Park SR, Choi BH, Min BH, Fetal Cartilage-derived Cells have Stem Cell Properties and are a Highly Potent Cell Source for Cartilage Regeneration, Cell transplantation (2015).

[21]. Fuchs JR, Terada S, Hannouche D, Ochoa ER, Vacanti JP, Fauza DO, Engineered fetal cartilage: structural and functional analysis in vitro, J Pediatr Surg 37(12) (2002) 1720–5. [PubMed: 12483640]

[22]. Responte DJ, Lee JK, Hu JC, Athanasiou KA, Biomechanics-driven chondrogenesis: from embryo to adult, FASEB J 26(9) (2012) 3614–24. [PubMed: 22673579]

[23]. Little CB, Ghosh P, Variation in proteoglycan metabolism by articular chondrocytes in different joint regions is determined by post-natal mechanical loading, Osteoarthritis and cartilage / OARS, Osteoarthritis Research Society 5(1) (1997) 49–62.

[24]. Williamson AK, Chen AC, Sah RL, Compressive properties and function-composition relationships of developing bovine articular cartilage, J Orthop Res 19(6) (2001) 1113–21. [PubMed: 11781013]

[25]. Williamson AK, Chen AC, Masuda K, Thonar EJMA, Sah RL, Tensile mechanical properties of bovine articular cartilage: variations with growth and relationships to collagen network components, J Orthop Res 21(5) (2003) 872–880. [PubMed: 12919876]

[26]. Haudenschild AK, Sherlock BE, Zhou X, Hu JC, Leach JK, Marcu L, Athanasiou KA, Nondestructive fluorescence lifetime imaging and time-resolved fluorescence spectroscopy detect cartilage matrix depletion and correlate with mechanical properties, European cells & materials 36 (2018) 30–43. [PubMed: 30051455]

[27]. Cissell DD, Link JM, Hu JC, Athanasiou KA, A Modified Hydroxyproline Assay Based on Hydrochloric Acid in Ehrlich's Solution Accurately Measures Tissue Collagen Content, Tissue engineering. Part C, Methods 23(4) (2017) 243–250. [PubMed: 28406755]

[28]. Bank RA, Beekman B, Verzijl N, de Roos JA, Sakkee AN, TeKoppele JM, Sensitive fluorimetric quantitation of pyridinium and pentosidine crosslinks in biological samples in a single high-performance liquid chromatographic run, J Chromatogr B Biomed Sci Appl 703(1–2) (1997) 37–44. [PubMed: 9448060]

[29]. Athanasiou KA, Agarwal A, Muffoletto A, Dzida FJ, Constantinides G, Clem M, Biomechanical properties of hip cartilage in experimental animal models, Clinical orthopaedics and related research (316) (1995) 254–66.

[30]. Brown WE, Hu JC, Athanasiou KA, Ammonium-Chloride-Potassium Lysing Buffer Treatment of Fully Differentiated Cells Increases Cell Purity and Resulting Neotissue Functional Properties, Tissue engineering. Part C, Methods 22(9) (2016) 895–903. [PubMed: 27553086]

[31]. Platt D, Bird JL, Bayliss MT, Ageing of equine articular cartilage: structure and composition of aggrecan and decorin, Equine Vet J 30(1) (1998) 43–52. [PubMed: 9458398]

[32]. Mow VC, Ratcliffe A, Structure and function of articular cartilage and meniscus, Second ed., Lippincott-Raven Publishers1997.

[33]. Ficklin T, Thomas G, Barthel JC, Asanbaeva A, Thonar EJ, Masuda K, Chen AC, Sah RL, Davol A, Klisch SM, Articular cartilage mechanical and biochemical property relations before and after in vitro growth, J Biomech 40(16) (2007) 3607–3614. [PubMed: 17628568]

[34]. Treppo S, Koepp H, Quan EC, Cole AA, Kuettner KE, Grodzinsky AJ, Comparison of biomechanical and biochemical properties of cartilage from human knee and ankle pairs, J Orthop Res 18(5) (2000) 739–48. [PubMed: 11117295]

[35]. Sah RL, Chen AC, Grodzinsky AJ, Trippel SB, Differential effects of bFGF and IGF-I on matrix metabolism in calf and adult bovine cartilage explants, Arch Biochem Biophys 308(1) (1994) 137–47. [PubMed: 8311446]

[36]. Verbruggen SW, Loo JH, Hayat TT, Hajnal JV, Rutherford MA, Phillips AT, Nowlan NC, Modeling the biomechanics of fetal movements, Biomech Model Mechanobiol 15(4) (2016) 995–1004. [PubMed: 26534772]

[37]. Flynn TW, Soutas-Little RW, Patellofemoral joint compressive forces in forward and backward running, J Orthop Sports Phys Ther 21(5) (1995) 277–82. [PubMed: 7787851]

[38]. Makris EA, Hu JC, Athanasiou KA, Hypoxia-induced collagen crosslinking as a mechanism for enhancing mechanical properties of engineered articular cartilage, Osteoarthritis and cartilage / OARS, Osteoarthritis Research Society 21(4) (2013) 634–41.

[39]. Makris EA, MacBarb RF, Responte DJ, Hu JC, Athanasiou KA, A copper sulfate and hydroxylysine treatment regimen for enhancing collagen cross-linking and biomechanical properties in engineered neocartilage, FA SEB J 27(6) (2013) 2421–30.

[40]. Makris EA, Responte DJ, Paschos NK, Hu JC, Athanasiou KA, Developing functional musculoskeletal tissues through hypoxia and lysyl oxidase-induced collagen cross-linking, Proceedings of the National Academy of Sciences of the United States of America 111(45) (2014) E4832–41. [PubMed: 25349395]

[41]. Akizuki S, Mow VC, Muller F, Pita JC, Howell DS, Manicourt DH, Tensile properties of human knee joint cartilage: I. Influence of ionic conditions, weight bearing, and fibrillation on the tensile modulus, J Orthop Res 4(4) (1986) 379–92. [PubMed: 3783297]

[42]. Eyre DR, The collagens of articular cartilage, Semin Arthritis Rheum 21(3 Suppl 2) (1991) 2–11. [PubMed: 1796302]

[43]. Morrison EH, Ferguson MW, Bayliss MT, Archer CW, The development of articular cartilage: I. The spatial and temporal patterns of collagen types, J Anat 189 (Pt 1) (1996) 9–22. [PubMed: 8771392]

[44]. Roddy KA, Prendergast PJ, Murphy P, Mechanical Influences on Morphogenesis of the Knee Joint Revealed through Morphological, Molecular and Computational Analysis of Immobilised Embryos, PloS one 6(2) (2011).

[45]. Mikic B, Isenstein AL, Chhabra A, Mechanical modulation of cartilage structure and function during embryogenesis in the chick, Annals of biomedical engineering 32(1) (2004) 18–25. [PubMed: 14964718]

[46]. Carter DR, Beaupre GS, Wong M, Smith RL, Andriacchi TP, Schurman DJ, The mechanobiology of articular cartilage development and degeneration, Clinical orthopaedics and related research (427) (2004) S69–S77. [PubMed: 15480079]

[47]. Kronenberg HM, Developmental regulation of the growth plate, Nature 423(6937) (2003) 332–6. [PubMed: 12748651]

[48]. Athanasiou KA, Eswaramoorthy R, Hadidi P, Hu JC, Self-organization and the self-assembling process in tissue engineering, Annual review of biomedical engineering 15 (2013) 115–36.

[49]. Pacifici M, Koyama E, Iwamoto M, Gentili C, Development of articular cartilage: what do we know about it and how may it occur?, Connective tissue research 41(3) (2000) 175–84. [PubMed: 11264867]

[50]. Oberlender SA, Tuan RS, Spatiotemporal profile of N-cadherin expression in the developing limb mesenchyme, Cell Adhes Commun 2(6) (1994) 521–37. [PubMed: 7743138]

[51]. Ofek G, Revell CM, Hu JC, Allison DD, Grande-Allen KJ, Athanasiou KA, Matrix development in self-assembly of articular cartilage, PloS one 3(7) (2008) e2795. [PubMed: 18665220]

[52]. Archer CW, Morrison EH, Bayliss MT, Ferguson MW, The development of articular cartilage: II. The spatial and temporal patterns of glycosaminoglycans and small leucine-rich proteoglycans, J Anat 189 (Pt 1) (1996) 23–35. [PubMed: 8771393]

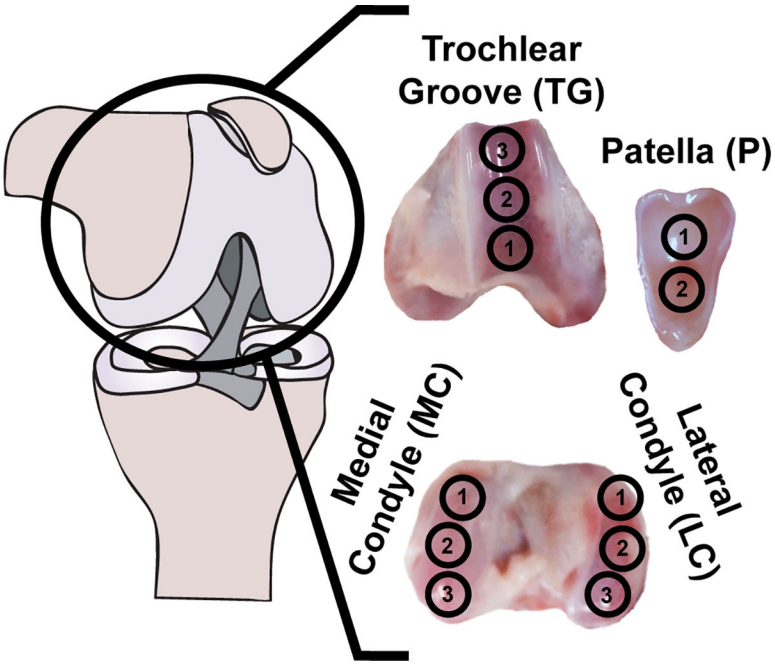

Fig. 1.

Topographical and regional overview: articular cartilage from 11 topographical locations across four regions of the fetal ovine stifle joint was characterized histologically, biochemically, and mechanically.

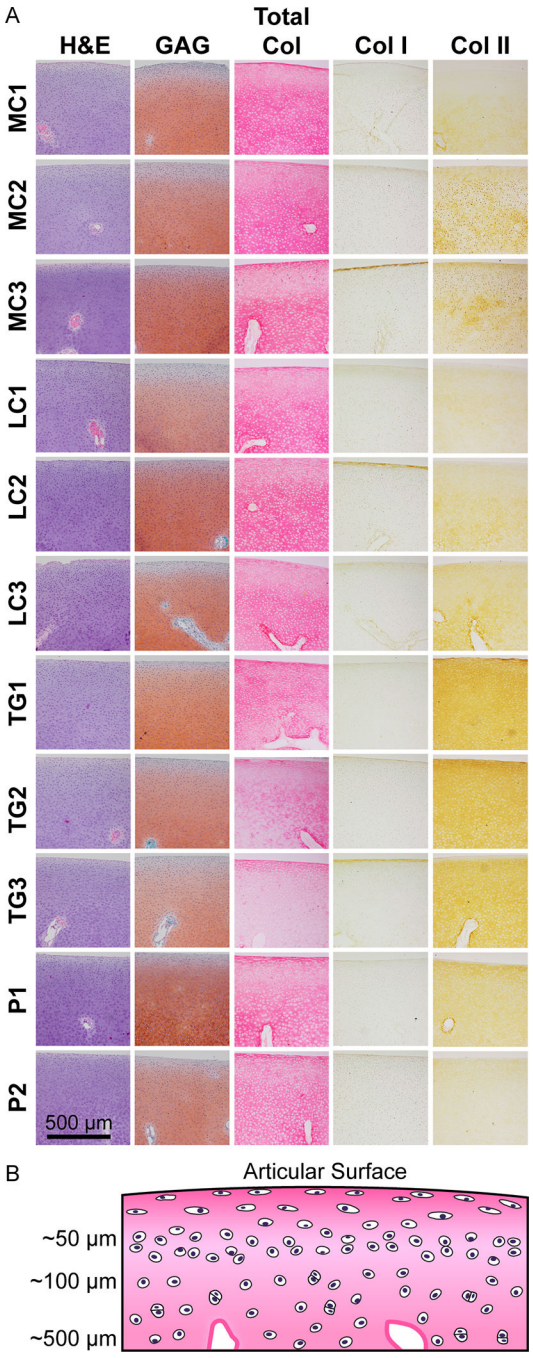

Fig. 2.

Histological and immunohistochemical evaluation: articular cartilage from three locations on the medial condyle (MC), three locations on the lateral condyle (LC), three locations on the trochlear groove (TG), and two locations on the patella (P) of the fetal ovine stifle were stained for GAG, total collagen, collagen I, and collagen II (A). Vasculature is present in every location. The LC stained most intensely for GAG, followed by the MC, TG, and P. Within each region, the locations with the most intense GAG staining were MC3, LC2, TG1, and P1, respectively. Collagen staining was similar in the MC and LC, but less intense in the

P and TG. Within each region, collagen staining was most intense at the MC2, LC2, TG1, and P2 locations, respectively. Collagen I staining was minimal in all locations. All locations stained for collagen II, but the TG and P stained most intensely. Within each region, collagen II staining was most intense at the MC2, LC3, TG1, and P1 locations, respectively. A schematic illustrating cell morphology and distance from the articular surface is shown (B).

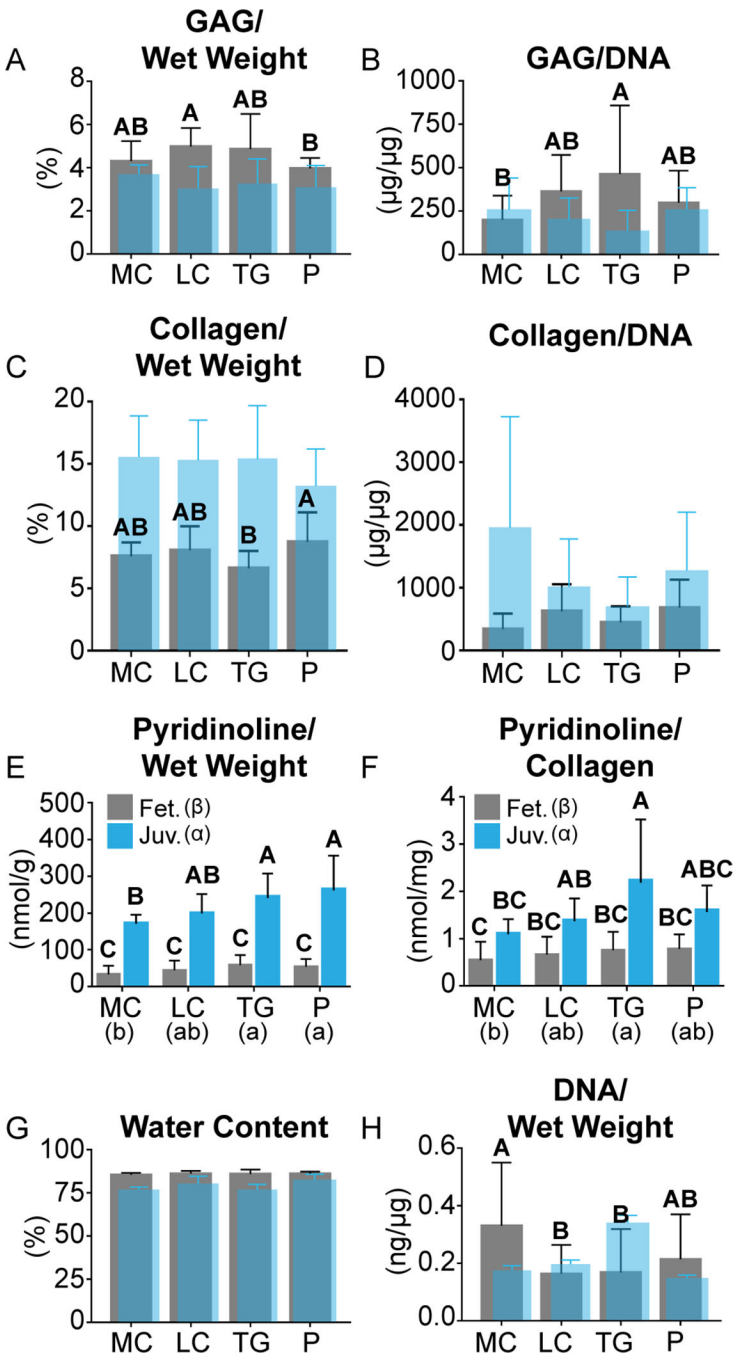

Fig. 3.

Biochemical Characterization: Biochemical contents of the fetal (fet.) ovine medial condyle (MC), lateral condyle (LC), trochlear groove (TG), and patella (P) are shown in gray. Historical values of biochemical content of juvenile (juv.) ovine cartilage from the same regions, except for pyridinoline content, are shown in translucent blue (A-D,G,H) [19]. Significantly different groups are indicated by labeling with different letters. Juvenile ovine pyridinoline/wet weight (E) and pyridinoline/collagen (F) contents, shown in blue, were calculated in this study. The LC contained the greatest GAG/ wet weight (A). The TG

contained the greatest GAG/ DNA (B). The P contained the greatest collagen/wet weight (C). There were no regional differences in collagen/DNA (D), pyridinoline/wet weight (E), pyridinoline/ collagen (F), or water content (G). The MC contained the greatest DNA/wet weight (H). Topographical biochemical data are available in Table 1. (For interpretation of the references to colour in this figure legend, the reader is referred to the web version of this article.)

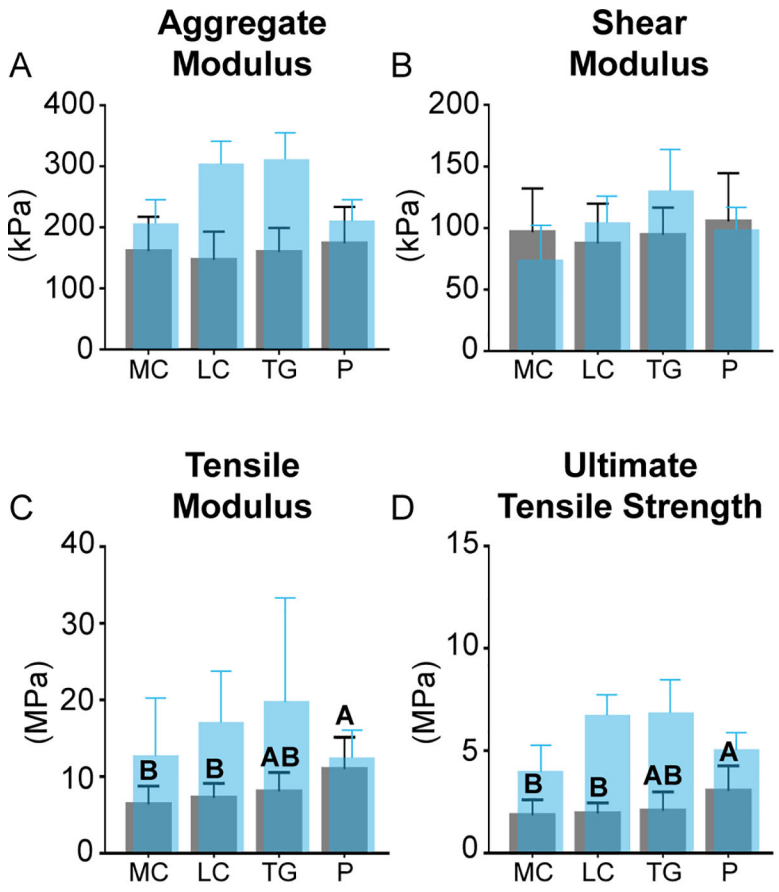

Fig. 4.

Mechanical characterization: mechanical properties of the fetal ovine medial condyle (MC), lateral condyle (LC), trochlear groove (TG), and patella (P) are shown in gray. Historical values of biochemical content of juvenile ovine cartilage from the same regions are shown in translucent blue [19]. No regional differences in aggregate modulus (A) or shear modulus (B) were observed. The P was stiffest (C) and strongest (D) in tension. Topographical mechanical data are available in Table 2. (For interpretation of the references to colour in this figure legend, the reader is referred to the web version of this article.)

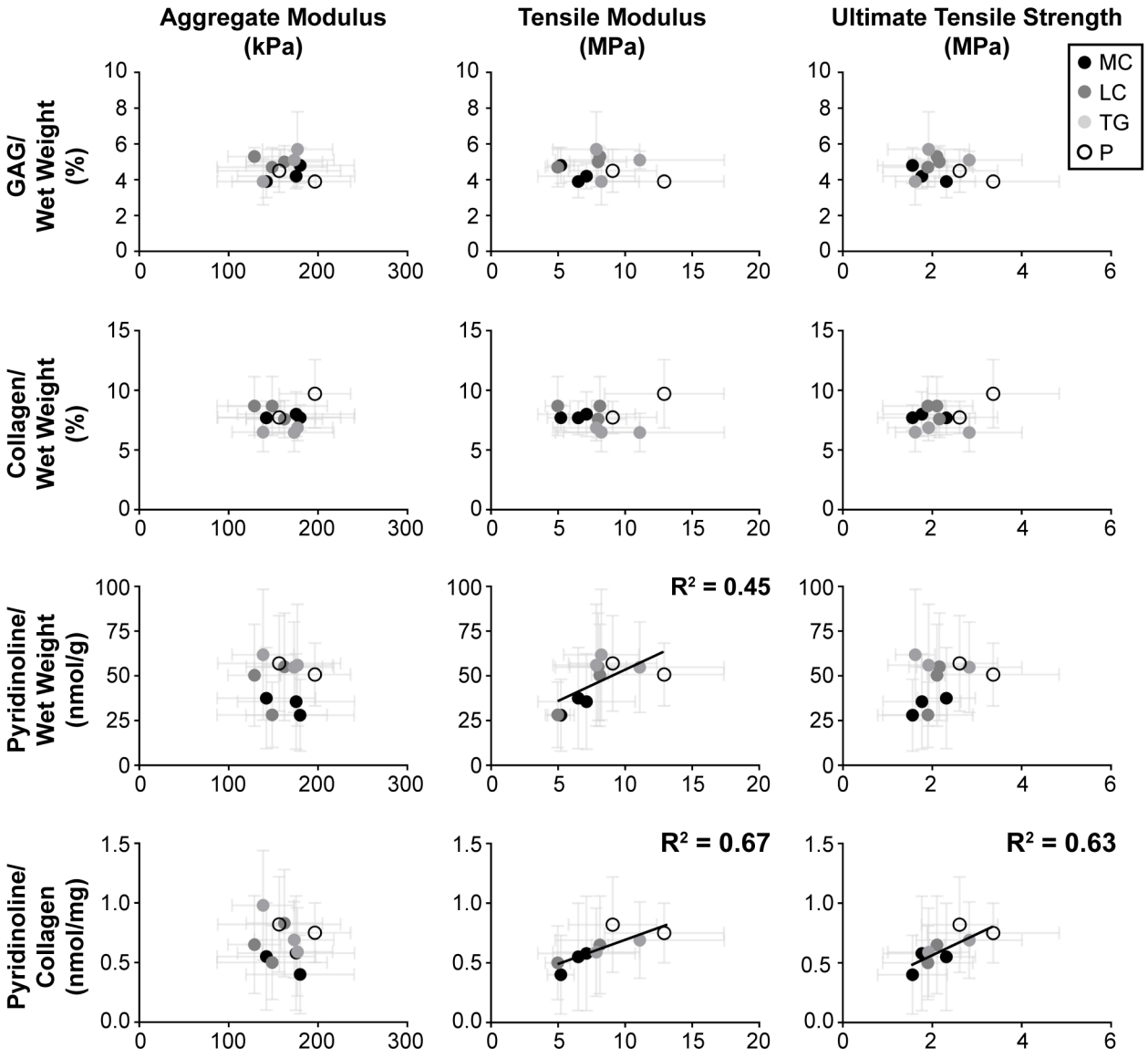

Fig. 5.

Structure-function correlations: correlations were tested among mechanical properties and biochemical contents. R_2 values are listed for significant correlations. The aggregate modulus, tensile modulus, and ultimate tensile strength were individually compared to the GAG/wet weight, collagen/wet weight, pyridinoline/wet weight, and pyridinoline/collagen, matched by location. Significant, positive correlations were observed between tensile modulus and both pyridinoline/wet weight and pyridinoline/collagen, as well as between ultimate tensile strength and pyridinoline/collagen.

Table 1 –

Topographical Biochemical Data:

Complete biochemical characterization data from 11 topographical locations are shown as mean ± standard deviation. Statistics were calculated amongst topographical locations within the same region.

Location		Water Content (%)	GAG/ Wet Weight (%)	GAG/ DNA (μg/μg)	Collagen / Wet Weight (%)	Collagen / DNA (μg/μg)	Pyridinoline / Wet Weight (nmol/g)	Pyridinoline / Collagen (nmol/mg)	DNA/ Wet Weight (μg/μg)
Medial Condyle	**1**	86 ± 1	3.9 ± 0.9	92 ± 32^{B}	7.7 ± 1.4	197 ± 101	22.5 ± 17.1	0.33 ± 0.27	0.49 ± 0.25
	2	86 ± 1	4.2 ± 0.7	230 ± 146^{AB}	8.0 ± 1.9	483 ± 380	21.3 ± 16.0	0.35 ± 0.29	0.26 ± 0.17
	3	85 ± 1	4.8 ± 1.0	292 ± 144^{A}	7.7 ± 1.1	496 ± 348	16.8 ± 12.1	0.24 ± 0.20	0.22 ± 0.14
Lateral Condyle	**1**	86 ± 2	4.7 ± 1.1	277 ± 147	8.7 ± 2.5	549 ± 343	16.9 ± 11.0	0.3 ± 0.18	0.23 ± 0.16
	2	86 ± 1	5.3 ± 0.5	355 ± 207	8.7 ± 2.5	542 ± 467	30.3 ± 17.1	0.39 ± 0.25	0.15 ± 0.05
	3	87 ± 2	5.0 ± 0.9	456 ± 262	7.6 ± 1.5	761 ± 519	33.0 ± 18.1	0.50 ± 0.27	0.17 ± 0.14
Trochlea r Groove	**1**	85 ± 3	5.7 ± 2.1^{A}	513±246	6.9 ± 1.1	511 ± 225	33.6 ± 20.4	0.35 ± 0.22	0.12 ± 0.09
	2	86 ± 2	5.1 ± 0.5^{AB}	640 ± 553	6.5 ± 1.6	938 ± 982	32.9 ± 15.2	0.41 ± 0.19	0.14 ± 0.11
	3	87 ± 3	3.9 ± 1.3^{B}	193 ± 89	6.5 ± 1.6	300 ± 192	37.1 ± 21.9	0.59 ± 0.28	0.25 ± 0.22
Patella	**1**	86 ± 1	4.5 ± 1.2	340 ± 220	7.7 ± 1.4	629 ± 437	34.2 ± 16.1	0.49 ± 0.24	0.21 ± 0.17
	2	86 ± 1	3.9 ± 0.3	246 ± 143	9.7 ± 2.9	725 ± 500	30.5 ± 10.6	0.45 ± 0.15	0.22 ± 0.16

Table 2 –

Topographical Mechanical Data:

Complete mechanical characterization data from 11 topographical locations are shown as mean ± standard deviation. Statistics were calculated amongst topographical locations within the same region.

Location		Aggregate Modulus (kPa)	Shear Modulus (kPa)	Per meability E-15 (m^4/N·s)	Tensile Modulus (MPa)	UTS (MPa)
Medial Condyle	1	142 ± 55	84 ± 36	4.9 ± 1.4	6.5 ± 0.1	2.4 ± 0.2
	2	176 ± 66	100 ± 37	6.4 ± 4.4	7.1 ± 3.6	2.4 ± 0.2
	3	180 ± 61	107 ± 34	7.5 ± 5.7	5.2 ± 1.0	2.4 ± 0.2
Lateral Condyle	1	149 ± 62	88 ± 42	4.9 ± 2.5	5.0 ± 0.9	2.4 ± 0.2
	2	129 ± 30	79 ± 23	5.4 ± 1.7	8.1 ± 0.6	2.4 ± 0.2
	3	162 ± 43	96 ± 32	4.2 ± 1.4	8.0 ± 2.1	2.5 ± 0.1
Trochlear Groove	1	177 ± 39	106 ± 21	4.4 ± 2.0	7.9 ± 3.2	2.2 ± 0.3
	2	173 ± 45	103 ± 26	4.1 ± 1.7	11.1 ± 6.3	2.1 ± 0.1
	3	139 ± 35	81 ± 19	7.1 ± 5.9	8.2 ± 2.8	2.1 ± 0.2
Patella	1	157 ± 69	95 ± 46	5.5 ± 3.0[A]	9.1 ± 3.3	2.4 ± 0.2
	2	197 ± 40	120 ± 25	2.4 ± 0.7[B]	12.9 ± 4.4	2.4 ± 0.2

Engineered neocartilage must be evaluated against healthy native cartilage and cell source tissue to determine its quality and degree of biomimicry. While fetal ovine cartilage has emerged as a promising and translationally relevant cell source with which to engineer neocartilage, it is largely non-characterized. Therefore, 11 locations across four regions (medial condyle, lateral condyle, trochlear groove, and patella) of the fetal ovine stifle were characterized. Importantly, locational and regional differences in functional properties were observed, and significant correlations of tensile properties to collagen and crosslink contents were detected, suggesting that functional adaptation begins *in utero*. This study provides a repository of quantitative information, clarifies the developmental order of cartilage functional properties, and informs future cartilage engineering efforts.